Iranian Journal of Hydrogen & Fuel Cell 1(2017) 53-68

Iranian Journal of Hydrogen & Fuel Cell

IJHFC

Journal homepage://ijhfc.irost.ir

Integration of a vanadium redox flow battery with a proton exchange membrane fuel cell as an energy storage system

H. A. Ozgoli[1], H. Yazdani[2*]

[1]Department of Mechanical Engineering, Iranian Research Organization for Science and Technology (IROST) Tehran, Iran
[2]Department of Chemical Engineering, Payame Noor University, Tehran, Iran

Article Information

Article History:

Received:
19 Jun 2017
Received in revised form:
23 July 2017
Accepted:
07 Aug 2017

Keywords

Vanadium redox battery
Proton exchange membrane fuel cell
Nernst equation
Transient model
Energy storage system

Abstract

The proton exchange membrane (PEM) fuel cell is a green energy producer which converts chemical energy to electricity in high yield. Alternatively, the vanadium redox flow battery (VRB) is one of the best rechargeable batteries because of its capability to average loads and output power sources. These two systems are modeled by Nernst equation and electrochemical rules. An effective energy generator should be able to operate with a new type of energy storage mechanism which would increase the capacity and stability of the comprehensive system using the proposed integrated system. Therefore, in this presented study a VRB as an energy storage system along with a PEM fuel cell has been modeled for peak shaving purpose. A transient model was created as a novel approach to predict cell operation condition, based on electrochemical equations and the battery equivalent circuit concept. Results showed that charging the VRB for one day with surplus produced electricity from the fuel cell will increase the total delivered power of the integrated system up to 50%.

1. Introduction

Nowadays the oil crisis is forcing us to find a substitute system for producing energy. One of these substituents is fosil fuels, but these are not sufficient; hence, we need to look forward to renewable energies and energy sources like ethanol and hydrogen. These renewable energy sources include the wind and solar. Using these substituents could reduce

*Corresponding Author's Fax: +98-21-56276632
E-mail address: h.yazdani@pnu.ac.ir

doi: 10.22104/ijhfc.2017.2281.1140

and solar. Using these substituents could reduce greenhouse gas emission, likeSO_x, NO_x, resulting in a cleaner environment. Fuel cells can operate with a very low level of noise [1, 2]; they transforms hydrogen into dc power. Fuel cells are commonly classified according to temperature and the type of electrolyte: (PEM, PAFC, MCFC, SOFC, AFC, RFC, and DMF). A proton exchange membrane (PEM) is a low-temperature fuel cell and vanadium redox flow batteries (VRB) have significant similarity with this kind of fuel cell. Their structures are shown in Fig. 1 and Fig. 2. Some of the main purposes of smart energy grids are preparing demand management, peak reduction, educating consumers and serving critical needs. On the other hand, integrated intermittent sources, such as renewable energy sources, perform suitably reliable for these grids. Fuel cells are a reasonable option to develop stable smart grids which have a green point of view. Principal advantages of fuel cells have been mentioned as follows [3]:

• Reliability: Clean, quiet power onsite; near 100% availability with a modular installation.

• Power Quality: Conditioned power; load following.

• Security: Local generation and local control; fewer, smaller, shorter connection/transmission lines.

• Affordability: Predictable pricing through contracts; scalable; heat capture; replaces the separate backup system.

Furthermore, fuel cells have significant privileges for smart grid projects. Some of their benefits are presented as follows:

• Prime power: Fuel cells operate 24/7, supplying some or all the customer load;

• Combined heat and power: Customer harvests some or all of the system heat;

• Grid Connected: Fuel cells offset a portion of the customer load;

• Backup power: Fuel cells supply all power or essential load in event of grid disruption;

• Independent: Fuel cells are completely disconnected from the grid.

Advances in the power electronics that convert DC power to AC have helped make redox flow battery storage systems increasingly reliable. Moreover, recent breakthroughs in advanced battery energy storage have shown the ability to deliver 5,000 to 10,000 charge/discharge cycles, or more. Advanced VRB systems that trim daily peaks (requiring at least 365 cycles per year) could last more than 10 years, and perhaps up to 30 years. In addition, there is the growing need for VRBs to store some types of renewable energy produced primarily during off-peak hours, and other types of green energy produced during shoulder hours, for subsequent on-peak consumption. These renewable applications will require 200 to 300 cycles per year. Also, when the renewables are not available, the battery could be used for arbitrage (buying low-cost energy at night and selling it during periods of high energy price) adding another 100 to 200 cycles per year. One of the benefits of energy modeling is the ability to predict quantities that are difficult or impossible to obtain through in situ experimental measurements.

In the previous studies of PEM fuel cell, the effect of temperature and capacity loss, voltage loss and ion diffusion and side effects have been studied [4, 5]. But the integration of vanadium redox flow batteries and proton exchange membrane fuel cell systems has been ignored. A VRB is suitable as an energy reservoir, whilst a PEM fuel cell is an efficient choice for reproducing energy. By integration, these two systems produce a clean and stable energy storage -VRB system- which can supply the essential energy of customers during nights or common peak hours.

In this study, a novel green integrated system has been presented, which contains a PEM fuel cell as a green energy generator along with VRB as clean energy storage. The consistency of these two systems, whose goal is a smart electricity grid, creates a unique opportunity to produce, store, provide stability, and control energy. In this study, a comprehensive integrated model of PEM and VRB has been built to consider the effects of reproducing electricity and time of storage in VRB systems. SOC parameter, concentration, and efficiency of polymer membranes have been investigated in the presented model.

2. System components

2.1. Proton exchange membrane fuel cell

The theory of fuel cells was first proposed by William Grave in the early 1836s and it was developed by inventions like the porous electrode, stack creation, Nernst equation, solid electrolyte and Nafion as a membrane. The first operative work was done by Francis Bacon [2].

In this kind of fuel cell, there is no combustion reaction and the fuel of this fuel cell is pure hydrogen. A proton exchange membrane (PEM) fuel cell is inclusive of a stack with a central membrane able to conduct protons, external layers that work as two electrodes and a set of layers that is pressed by two conductive plates. The plates contain channels in which the reactants flow, the structure of these layers are porous and partially hydrophobic. The cathode feed enters the air and hydrogen is fed to the anode. By a reaction of hydrogen and oxidant, chemical energy converts to electrical energy in the anode hydrogen which will release electrons. The electrons are transferred to the cathode and the current will be established, hydrogen traverses the membrane and produces water with a oxidant reaction [1]. One of the disadvantages of using this system is carbon dioxide production. This can be reduced by solar cells electrolyzing resulting in a zero level of emission.

Sources of voltage drop in PEM fuel cells are:

1) activation polarization, 2) ohmic polarization, and 3) concentration polarization. The PEM fuel cell's voltage losses result in: activation losses, internal current losses, resistive losses, nad mass transport or concentration losses. There are some actions that decrease the voltage drop in PEM fuel cells, such as increasing temperature, increasing pressure, increasing hydrogen or oxygen concentration, increasing electrode effective surface, reducing electrolyte thickness to possible limitation, using electrodes with the highest possible electroconductivity, and using good design for the plates and cell connections or "connection modification" [6, 7].

PEM fuel cells have high yields (45%) and they work at low temperatures. A powerhouse utilizing this technique has low emission gas, but they are expensive and have a low service life.

The reactions in this fuel cell are as below [1]:

The chemical reaction at the anode:

$$H_2 \rightarrow 2H^+ + 2e \tag{1}$$

The chemical reaction at the cathode:

$$2H^+ + \frac{1}{2}O_2 + 2e^- \rightarrow H_2O \tag{2}$$

Overall reaction:

$$H_2 + \frac{1}{2}O_2 \rightarrow H_2O + 2e + Q - \frac{3}{2}RT \tag{3}$$

Where,

3/2 RT is Water liquefy energy.

As explained in previous research, a fundamental PEM fuel cell model consists of five principles of conservation: mass, momentum, species, electric charge, and thermal energy. These five balance equations are summarized in Table 1 with their source terms identified for a fuel cell.

Energy balance in a PEM fuel cell can be indicated by the following equations. In other words, inputs are chemical energies which might be explained by enthalpy, heat or Gibbs energy.

$$G = H - T.S,\ \Delta G = \Delta H - T.\Delta S \tag{4}$$

$$\Delta G = \Delta H - T.\Delta S \tag{5}$$

$$\Delta G = \Delta H_0 - \frac{T}{T_0}\left(\Delta H_0 - \Delta G_0\right) - \Delta C_p.T.\left[Ln\frac{T}{T_0} + \left(\frac{T}{T_0} - 1\right)\right] \tag{6}$$

Where T_0=298 K and P_0=1 atm;

$$\Delta C_p = C_p\left(H_2O\right) - C_p\left(H_2\right) - \frac{1}{2}C_p\left(O_2\right) \tag{7}$$

$$E_{rev} = \frac{-\Delta G}{n.F} = \frac{-\Delta G}{\left(4 \times 46.487 \times n_o\right)} \tag{8}$$

Where,
T.ΔS is available to heat in a reversible reaction.
By subtracting catalytic and resistive losses from the reversible electrochemical cell, the steady-state cell voltage is calculated. This concept has been expressed in Eq. (9):

$$E_{cell}=E_{rev}-\eta_{anode}-\eta_{cathode}-\eta_{ohmic}-\eta_{interface} \quad (9)$$

The reversible cell potential (E_{rev}) can be found from the well-known thermodynamic relation:

(10)

$$E_{rev}=1.2291-8.4517\times10^{-4}(T-298.15)+4.3080\times10^{-5}\ T\ (Ln_{PH2}+0.5Ln_{PO2})$$

Where P_{O2} and P_{H2} are the partial pressures of hydrogen and oxygen, respectively, at the catalysis interface.
In PEM fuel cells the dominant factor is the ohmic losses, due to the resistance of the wiring and the resistance of the imperfect electrodes. In most cases, the ohmic drop or the ohmic over potential is given by Eq. (11):

$$\eta_{ohm}^{proton}=-I\times R^{proton} \quad (11)$$

And R^{proton} is the proton membrane resistance.
Modeling overpotential caused by the interaction of different phases, solid and gas interface between electrode and membrane, is complex and depends on many parameters. Thus, a simplified empirical equation proposed by Kim et al. [8] has been adopted in this study:

$$\eta_{interface}=m\cdot\exp(n\times J) \quad (12)$$

The overpotential equation has been explained by the Butler-Volmer approach, which is used for the electrodes in general form. Entropy changes cause heat generation in the cell, which is consequent of irreversibility due to the activation overpotential:

$$q=\left[\frac{T(-\Delta S)}{nF}+\eta_{act,c}\right]i_c \quad (13)$$

The local current density distribution in the catalyst layers has been modeled by the Butler-Volmer equation:

$$i_c=i_{O,c}^{ref}\left(C_{O_2}/C_{O_2}^{ref}\right)\left[exp\left(\left(\alpha_a F/RT\right)\eta_{act.c}\right)+exp\left(\left(\alpha_c F/RT\right)\eta_{act.c}\right)\right] \quad (14)$$

$$i_a=i_{O,a}^{ref}\left(C_{H_2}/C_{H_2}^{ref}\right)\left[exp\left(\left(\alpha_a F/RT\right)\eta_{act.a}\right)+exp\left(\left(\alpha_c F/RT\right)\eta_{act.a}\right)\right] \quad (15)$$

Mass, momentum, species and charge conservation principles for PEM fuel cells are as below [24]:

$$\nabla.(\varepsilon\rho\vec{u})=0$$
$$\frac{1}{\varepsilon^2}\nabla.(\rho\vec{u}\vec{u})=-\nabla p+\nabla.(\mu\nabla\vec{u})+S_u \quad (16)$$

$$S_u=-\frac{\mu}{k}\vec{u} \quad (17)$$

$$\nabla.(\vec{u}C^i)=\nabla.(D^{(I,eff)}\nabla C^i)+S_k=0 \quad (18)$$

In the above u is the velocity, ρ is the density and ε is the porosity coefficient.
Where P is the pressure, μ is the viscosity, S_u is for applying Darcy law atlow rates, K is the diffusion in porous(layers/membranes?), C^i is the concentration of elements, and $D^{I,eff}$ is the dispersion coefficient [9].

2.2.Vanadium Redox Flow Battery

The idea of a redox flow battery was first proposed by NASA for energy storage in the early 1970s and advanced by projects on the advanced battery electric power storage system by NEDO in Japan [10]. This type of battery was first invented by Skyllas-Kazacos and co-workers at the University of New South Wales (UNSW) in the mid-1980s [11, 12]. The application of these batteries in the military industry, mobile power systems, recycle systems, powerhouse industries extended its use. A VRB battery is inclusive of two reservoirs for electrolyte solution preservation and energy is stored in these solutions, it has two half cells which are separated by a membrane. Liquid electrolytes are stored in external tanks and circulated through a cell tank where the

Table 1. Governing equations of PEM fuel cell with source terms.

	Conservation equations	Diffusion layers	Catalyst layers	membrane
Mass	$\partial(\epsilon\rho)/\partial t+\nabla(\rho\vec{u})=S_m$		$\sum_k M_k S_k + M_{H_2O}\nabla\left(D_{W,M}\nabla C_{H_2O}\right)$	
Momentum	$1/\epsilon\left[\partial(\rho\vec{u})/\partial t+1/\epsilon\nabla(\rho\vec{u}\vec{u})\right]$ $=-\nabla p+\nabla\tau+S_u$	$S_u=(-\mu/K)\vec{u}$	$S_u=(-\mu/K)\vec{u}$	$\vec{u}=0$
Species	$\partial(\epsilon C_k)/\partial t+\nabla(\vec{u}C_k)=$ $\nabla\left(D_k^{eff}\nabla C_k\right)+S_k$		$S_k=-\nabla\left[(n_d/F)i_e\right]$ $-(S_k J/nF)$	
Charge	$\nabla(\kappa^{eff}\nabla\Phi_e)+S_\Phi=0$ $\nabla(\sigma^{eff}\nabla\Phi_e)+S_\Phi=0$		$S_\Phi=j$	$S_k=-\nabla\left[(n_d/F)i_e\right]$
Energy	$\partial\left[(\rho c_p)_m T\right]/\partial t+\nabla(\rho c_p\vec{u}T)$ $=\nabla\left(\kappa^{eff}\nabla T\right)+S_T$		$S_T=j\left[\eta+T(dU_0/dT)\right]$ $+\left(i_e^2/\kappa^{eff}\right)$	$S_T=i_e^2/\kappa^{eff}$

Electrochemical reaction $\sum_k M_k S_k = ne^-$, where M_k ≡ chemical formula of species k, S_k ≡ stoichiometry coefficient, and n ≡ number of electrons transferred. In PEM fuel cells there are (anode) H_2-$2H^+$=$2e^-$ and (cathode) $2H_2$ O-O_2-$4H^+$=$4e^-$.

energy conversion process occurs due to electrochemical reduction-oxidation reactions [13, 14]. VRB has unique applications such as renewable energy storage, peak shaving, and electric utility load leveling. In this battery, the electrolyte is used for energy storage, the stack is used as an energy transformer and a pump circulates the electrolyte. The role of the membrane is to keep the solutions separate and allow the transfer of H+ protons, the reaction is reversible and the battery can be charged and discharged [15]. The advantage of this system is high yield, unlimited longevity, low environmental effects and a lack of chemical decreasing because of corrosion. Equations in positive and negative electrodes are as below.

At the positive electrode:

$$VO^{2+}+H_2O \xleftrightarrow{\text{charge and discharge}} VO_2^{+}+2H^{+}+e^{-}, \quad E_0=1V \tag{19}$$

At negative electrode:

$$V^{3+}+e^{-} \xleftrightarrow{\text{charge and discharge}} V^{2+}, \quad E_0=-0.26V \tag{20}$$

Generally, this system operates under the isothermal

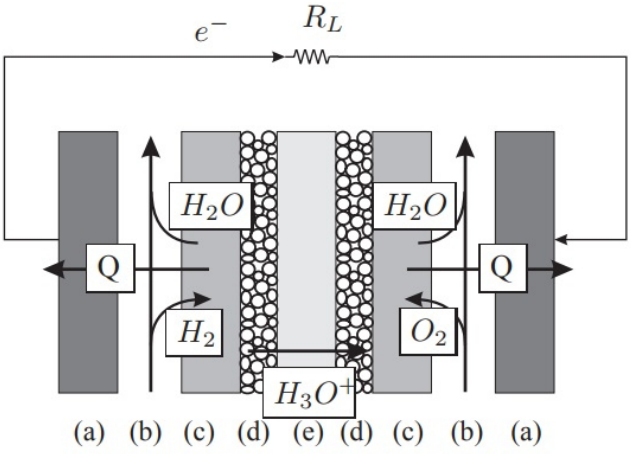

Fig. 1. The structure of a PEM fuel cell a) Bipolar plate, b) Gas flow channel, c) Electrode layer, d) Catalyst layer, and e) polymer layer.

condition and is described by mass, momentum, species and charge conservation principles. Under the above assumption, the following equations present the conservation as below [16, 17]:

Continuity:

$$\nabla.\vec{v}=0 \tag{21}$$

Momentum conservation:

$$\frac{\mu}{K}\vec{v}=-\nabla P \tag{22}$$

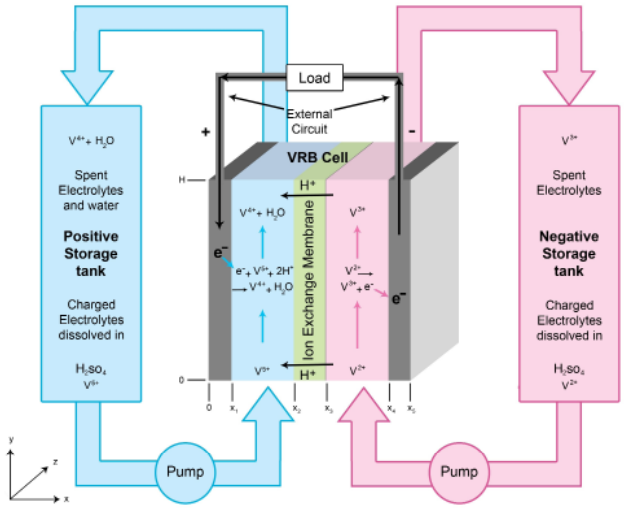

Fig. 2. The Schematic of the VRB system and modeling domains.

Species conservation:

$$\vec{v}\nabla c_i - D_i^{eff}\nabla^2 c_i = S_i \tag{23}$$

Charge conservation:

$$\nabla.\vec{i_s} = -\nabla.\vec{i_l} = -\sigma_s^{eff}\nabla^2\phi_S = -K_l^{eff}\nabla^2\phi_l = S_\phi \tag{24}$$

Where:

$\vec{v}$ refers to the intrinsic fluid velocity vector; P refers to the fluid pressure, c_i refers to the concentration of species i, i∈{V^{2+},V^{3+}, VO_2^+, VO^{2+}, H^+}; S_i, denotes the source term for species i; ϕ_S and ϕ_l denote the potential of the solid and liquid phase, respectively; S_ϕ, denotes the source term for charge conservation [18].

Table 1 lists the source terms for species conservation and charges conservation in the positive and negative electrodes. The source terms in the membrane are all set to zero. Where E_{Pos} and E_{neg} can be estimated from the relevant Nernst equations [19]:

$$E_{Pos} = E_{Pos}^0 + \frac{RT}{F}Ln\left(\frac{c_5}{c_4}\right) \tag{25}$$

$$E_{neg} = E_{neg}^0 + \frac{RT}{F}Ln\left(\frac{c_3}{c_2}\right) \tag{26}$$

The values of the equilibrium potentials E_{Pos}^0 and E_{neg}^0 have been categorized in Table 2. The vanadium concentrations at the surface of the positive electrode will be [20]:

$$c_4^S = \frac{B_{Pos}c_5 + (1+B_{Pos})c_4}{1+A_{Pos}+B_{Pos}} \tag{27}$$

$$c_5^S = \frac{B_{Pos}c_4 + (1+B_{Pos})c_5}{1+A_{Pos}+B_{Pos}} \tag{28}$$

Where, A_{Pos} and B_{Pos} have the following expressions [17, 20, 21]:

$$A_{Pos} = \frac{k_{Pos}}{k_{m,Pos}}(c_4)^{\alpha_{Pos}c^{-1}}(c_5)^{\alpha_{Pos,a}}\exp\left(\frac{\alpha_{Pos,a}F\eta_{Pos}}{RT}\right) \tag{29}$$

$$B_{Pos} = \frac{k_{Pos}}{k_{m,Pos}}(c_4)^{\alpha_{Pos,c}}(c_5)^{\alpha_{Pos,a}^{-1}}\exp\left(-\frac{\alpha_{Pos,c}F\eta_{Pos}}{RT}\right) \tag{30}$$

The mass transfer coefficient is approximately calculated by [17]:

$$k_{m,Pos} = 1.6\times10^{-4}\left|\vec{v}\right|^{0.4} \tag{31}$$

Similar expressions are applied to the species at the negative electrode as follows:

$$c_2^S = \frac{B_{neg}c_3 + (1+B_{neg})c_2}{1+A_{neg}+B_{neg}} \tag{31}$$

$$c_3^S = \frac{A_{neg}c_2 + (1+A_{neg})c_3}{1+A_{neg}+B_{neg}} \tag{32}$$

3. Model assumption

3.1.Model assumption for VRB

Several assumptions have been considered, in order to develop the VRB model as follows [22, 23]:

• The fluid flow has been considered incompressible. It has been assumed that the fluid density remains unchanged during the operation.

• The electrode, electrolyte and membrane physical characteristics have been considered isentropic and homogenous and their changes in different directions have been eliminated.
• Isothermal condition exists in all directions.
• Side reactions, such as oxygen and hydrogen changes, have not been taken into account.
• Effects caused by gravity have been eliminated.
• Effects caused by water permeation to the membrane have been eliminated.
• The model has been considered in a stationary state.
• The electrode materials have been made of carbon.
• The membrane material has been made of Nafion.

3.2.Model assumption for PEM fuel cell

Several assumptions have been considered to develop the VRB model as follows [24]:
• Ideal gas mixture.
• Incompressible and laminar flow due to small pressure gradients and flow velocities.
• Isotropic and homogeneous electrodes, catalyst layer and membrane.
• Contact cell temperature.
• Negligible ohmic potential drop in the electronically conductive solid matrix of the porous electrodes and catalyst layer.

4.Structure of PEM fuel cell integrated with VRB system

First, the VRB model, which stores the produced energy from PEM fuel cell, was developed, Two reactions occured on two sides of the membrane during the discharge process. The equations of reactions are as below [25, 26]:

$$VO_2^+ + 2H^+ + e^- \leftrightarrow VO^{2+} + H_2O$$
$$V^{2+} \leftrightarrow V^{3+} + e^- \qquad (34)$$
$$V^{(2+)} + VO^{(2+)} + 2H^+ ? VO^{(2+)} + V^{(3+)} + H_2O$$

In the discharging process, the electrons from the anode enter the cathode and pass the external circuit; in the charging process the movement of the electrons reverses. Reduction and oxidation occur in the anode and cathode, respectively. The positive half-cell has V^{2+} and V^{3+} ions and the negative one has V^{4+} and V^{5+} ions.
As it has been shown in Figs. 3 and 4, two different modes were considered. In thecharging mode, the excess energy produced from the PEM fuel cell will be stored in the VRB. When it is discharged, the system current is disconnected, the electricity load uses the stored energy in the VRB system and the VRB acts as a resource of electricity. This will increase energy efficiency and assurance capability of the grid.
The electricity is produced by the reduction reaction of vanadium; some of this electricity is used by a connected consumer. Water and heat will be produced in the PEM fuel cell and they should be omitted from the system.
PEM system produces electricity whereas the vanadium flow battery is a storage system. In a VRB battery you can increase the stored energy by

Table 2. Considered kinetic parameter in VRB model gas.

Parameter	Value	Unit	Description
k_{Pos}	2.50×10^{-8}	$m.s^{-1}$	Rate constant, positive reaction
k_{neg}	7.00×10^{-8}	$m.s^{-1}$	Rate constant, negative reaction
$\alpha_{Pos,a}$	0.55	-	Anodic transfer coefficient, positive reaction
$\alpha_{Pos,c}$	0.55	-	Cathodic transfer coefficient, positive reaction
$\alpha_{neg,a}$	0.45	-	Anodic transfer coefficient, negative reaction
$\alpha_{neg,c}$	0.45	-	Cathodic transfer coefficient, negative reaction
E_{pos}^{0}	1.004	V	Standard potential, positive reaction
E_{neg}^{0}	-0.255	V	Standard potential, negative reaction

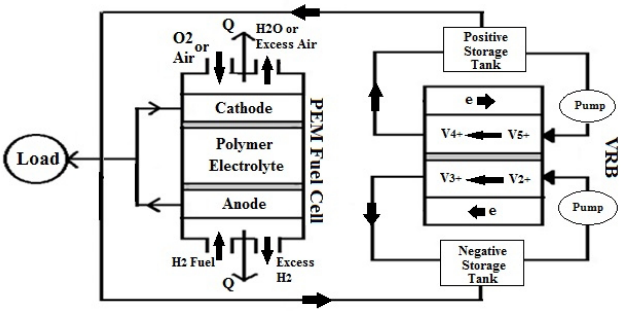

Fig. 3. The structure of PEM and VRB system connected (charged)

increasing the charged volume of the electrolyte without changing the dimensions of stack, but you have to increase the whole dimension of an acid-plumb or nickel-cadmium battery to increase the power and yield , because the electrodes and electrolyte are in one place [27, 28]. By incorporating the PEM and VRB there is the possibility of charging one system while another system is vacating, but a controlled system is required to make this possible. It should be noted that the membrane of the two systems is polymeric and their diameter is small. The polymeric membrane can be a poly (Ether Sulfone) or Sulfonated Poly (Ether Ether Ketone) blend [29, 30].

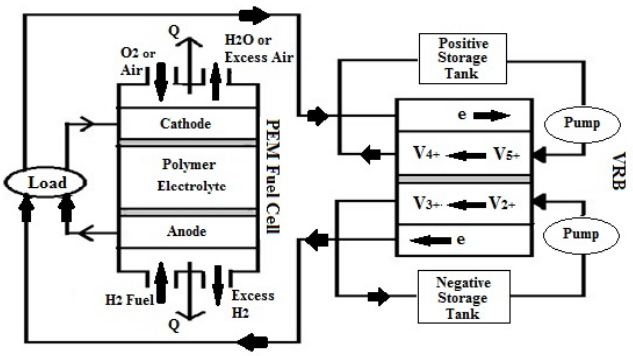

Fig. 4. The structure of PEM and VRB system connected (discharged)

According to previous statements, the surplus produced energy of the PEM fuel cell is send to the VRB system to store for use in peak hours. Therefore, the total electrical capacity of the grid will be increased using the proposed integrated system.

5.Initial and Boundary Conditions

Boundary conditions are required at all boundaries of the computational domains, as well as at internal interfaces.

5.1.Boundary Conditions for Charge Conservation

Since the battery is operated in the galvanostatic mode the flux conditions for potential distribution of the porous electrode are as follows (during charge) [31]:

$$-\sigma_s^{eff}\nabla\phi_s.\vec{n} = I_{app}\left(x=0,\ x=x_1\right) \quad (35)$$

$$-\sigma_s^{eff}\nabla\phi_s.\vec{n} = -I_{app}\left(x=x_4\right) \quad (36)$$

$$-\sigma_s^{eff}\nabla\phi_s.\vec{n} = I_{app}\left(x=x_2,\ x=x_3, y=0, y=H\right) \quad (37)$$

The charge leaving the solid phase is balanced by the charge entering the electrolyte where,I_{app}, is the applied current density. For discharge the signs are reversed. Therefore, the boundary conditions on the potential distribution for electrolyte during charge are specified as [32-34]:

$$-\kappa_l^{eff}\nabla\phi_l.\vec{n} = -I_{app}\left(x=x_2\right) \quad (38)$$

$$-\kappa_l^{eff}\nabla\phi_l.\vec{n} = I_{app}\left(x=x_3\right) \quad (39)$$

$$-\kappa_l^{eff}\nabla\phi_l.\vec{n} = 0\left(x=0, x=x_1,\ x=x_4, y=0, y=H\right) \quad (40)$$

For discharge the signs are reversed.

5.2.Boundary condition for momentum balance

Where the velocity boundary conditions are used at the inlets, pressure boundary conditions are used at the outlets and on all walls, the no-slip boundary condition is applied to the momentum equations. The detailed expressions are as follows (for VRB):

$$\upsilon_y=\upsilon_{in}\ (y=0) \quad (41)$$

$P=P._{Out}(y=H)$ (42)

$$\nabla P.\vec{n}=0\left(x=x_1,\ x_2,x_3,x_4\right) \tag{43}$$

At the outlets (y = H) [34]:

$$-D_i^{eff}\nabla c_i.\vec{n}=0 \tag{44}$$

When all the other boundaries are set to walls it means that the fluxes are zero:

$$\left(-D_i^{eff}\nabla c_i+c_i\vec{v}\right).\vec{n}=0 \tag{45}$$

The diffusion of vanadium ions across the membrane has a significant impact on the capacity of the VRB. Differential rates of diffusion of the vanadium ions from one half-cell into the other will facilitate self-discharge reactions, leading to an imbalance between the state-of-charge of the two half-cell electrolytes and a subsequent drop in capacity [35].

$$\begin{aligned}&\frac{d^2\left[V^{2+}\right]_{cell}}{dt^2}=-\left\{Q\left(\frac{1}{V_{tank}}+\frac{1}{V_{cell}}\right)-\frac{1}{Q}\frac{dQ}{dt}\right\}\\&\frac{d\left[V^{2+}\right]_{cell}}{dt}\mp\frac{1}{V_{cell}F}\frac{dI}{dt}\mp\left(\frac{Q}{V_{tank}}-\frac{1}{Q}\frac{dQ}{dt}\right)\frac{1}{V_{cell}}\frac{I}{F}\end{aligned} \tag{46}$$

The boundary conditions ina PEM fuel cell is based on the concentration profile in the catalyst layer, these boundary conditions are required only at the external surfaces of the computational domain due to the single domain formulation used. There is a no-flux condition except for the inlets and outlets of the flow channels. At the fuel and oxidant inlets, the following condition is as below [36]:

$$u_{(in,anode)}=U^0,u_{(in,anode)}=U_+^0 \tag{47}$$

$$\begin{aligned}&X_{H_2,anode}=X_{H_2,-},\ X_{O_2,cathode}=X_{o_2,+},\ X_{H_2O,anode}\\&=X_{H_2O,-},\ X_{H_2O,cathode}=X_{H_2,+}\end{aligned} \tag{48}$$

In the above equations, u is the velocity vector (cm/s), U is the inlet velocity (cm/s) and X is the mole fraction of species.

As it is shown in Fig. 2, VRB has a negative and positive porous electrode, stacks separated by a membrane in which the reaction occurs, and two storage tanks. The model includes a battery voltage source, a unidirectional parallel-connected equivalent internal resistance, a RC parallel circuit and a temperature prediction module. The parallel diodes have different charge/discharge resistances, R_C and R_d. The predicted overall stack voltage during discharge can be determined by Eq. (49) [29, 37]:

$$\begin{aligned}&U_{battery}=E\left(SOC,T\right)-V_h-V_r=\\&E_0+\frac{\partial E_0}{\partial T}\Delta T+N\frac{2mRT}{F}\ln\left(\frac{SOC}{1-SOC}\right)-V_r-R_dI\end{aligned} \tag{49}$$

The predicted overall stack voltage during charge can be determined by Eq. (50),

$$\begin{aligned}&U_{battery}=E\left(SOC,T\right)+V_h+V_r=\\&E_0+\frac{\partial E_0}{\partial T}\Delta T+N\frac{2mRT}{F}\ln\left(\frac{SOC}{1-SOC}\right)+V_r+R_dI\end{aligned} \tag{50}$$

When it reaches the equivalent state of charge (SOC) charging will be terminated, SOC means the state of charge was estimated by the residual V(III) reactant concentration:

$$SOC=1-\frac{C_{3,av}}{C_3^0} \tag{51}$$

The state of charge of the system can be monitored by measuring the OCV using Nernst Equations [23]:

$$\begin{aligned}&OCV=ROCV-\Delta\upsilon_{i=0}=E_{cell}=\\&E_{cell}^0+\frac{RT}{n_VF}Ln\frac{\left[V^{5+}\right]\left[V^{2+}\right]\left[H^+\right]^2}{\left[V^{4+}\right]\left[V^{3+}\right]}\\&[V^{(5+)}]=[V^{(2+)}]\text{and}[V^{(4+)}]=[V^{(3+)}]\\&[V^{(5+)}]\alpha SOC\text{and}[V^{(4+)}]\alpha 1-SOC\\&[V^{(5+)}]=[V^{(5+)}]_i(SOC^*)\\&[V^{(4+)}]=[V^{(4+)}]_i(1-SOC^*)\end{aligned} \tag{52}$$

Therefore at 25°C,

$$\begin{aligned}&E_{cell}=E_{cell}{}^0+\frac{RT}{(n_{v^F})}Ln[H^+]^2+\frac{RT}{(n_{v^F})}Ln\frac{[SOC^*]^2}{[1-SOC^*]^2}=\\&E_{cell}{}^{0,*}+\frac{RT}{(n_{v^F})}Ln\frac{[SOC^*]^2}{[1-SOC^*]^2}\end{aligned} \tag{53}$$

where $E_{cell}^{0,*}$ is the cell potential at 50% SOC and-SOC* is the state of charge expressed as a fraction.
Standard potential E^0 is dependent with temperature and has a relationship with Eq. (54),

$$\frac{\partial E^0}{\partial t} = \frac{1}{nF}\left(\frac{\partial \Delta G}{\partial T}\right) \quad (54)$$

where ΔG refers to the standard Gibbs free enthalpy and the values.
SOC=0 corresponds to no charge and SOC=1 corresponds to a full charge. Voltage with zero level current density condition is an open circuit voltage. The quantity of $C_{3,av}$ corresponds to average V(I-II) concentration. In this battery there are some crossovers that result in capacity losses, the crossovers mean the undesired transport of active vanadium species across the membrane; this capacity loss results in significant loss of available stored energy and the long-term performance of this systems will be limited [38]. This anadium crossover initiates reversible side reactions in the electrolytes and decreases the columbic efficiency during cycling.
A typical PEM fuel cell has a V-I characteristic at room temperature and normal air pressure, as shown in Fig. 2. The output voltage of the PEM fuel cell is defined by equation (55) [39]:

$$E = N\left(E_0 + \frac{RT}{nF}\ln\left\{\frac{P_{H_2}\left(\frac{P_{O_2}}{P_{std}}\right)^{1/2}}{P_{H_2O_C}}\right\} - L\right) \quad (55)$$

Voltage losses (L) in the PEM fuel cell can be calculated by Eq. (56):

$$L = \frac{RT}{\propto nF}\ln\left(\frac{i+i_n}{i_0}\right) + r\left(i+i_n\right) - \frac{RT}{nF}\ln\left(1-\frac{i+i_n}{i_L}\right) \quad (56)$$

In a model for a PEM fuel cell, the efficiency of the cell is attributed to the produced waste heat. The amount of the heat is estimated from the difference between the thermoneutral voltage and cell output voltage. The reversible voltage E_{rev}, is calculated from a modified Nernst equation with extra terms to account for the deviation from standard temperature and concentration [40]:

$$E_{rev} = \frac{\Delta G}{2F} + \frac{\Delta S}{2F}\left(T - T_{ref}\right) + \frac{RT}{2F}\ln\left[\left(\frac{C_{H_2}}{C_{H_2,ref}}\right)\left(\frac{C_{O_2}}{C_{O_2,\,ref}}\right)^{1/2}\right] \quad (57)$$

6. Results and discussion

6.1. Voltage and current changes

Potential of electricity decreases in the discharging cycle and increases in charging, because of electrical reactions and also the electrical current production in the battery cells. The electrical potential ascends while charging and descend while discharging.
The rate of electrolyte potential from negative to positive side at a certain times of cell operation will decrease, the electric potential in discharging on the negative side will be generated and the maximum amount of potential is 0.25 V on the negative side. At the beginning of the discharge cycle, the maximum voltage of the cell has been calculated at about 1.37 V. To reduce the voltage change the structure of electrodes should be improved, for example an electrolyte with high conductivity should used. Uniform voltage distribution can be achieved In PEM fuel cells without uniform distribution of reactant flow and temperature. The temperature distribution will increase the cell voltage along the stack, while the flow non-uniformity will cause the cell voltage to decrease along the stack.
According to Figs. 5 and 6, the need to manage energy consumption and production can be solved by intelligent systems and control schemes. In addition, the proposed PEM fuel cell, the VRB, becomes a viable tool in a smart grid operator's overall energy management model and the side benefit is a robust, long run-time, clean backup power system.

Table 3. Voltage drop sources and actions to reduce them.

Voltage drop	Acts to reduce voltage drop
Activation losses	Reduction in battery temperature;
	Using proper catalysts;
	Increasing surface of electrode;
	Increasing concentration of reactants;
	Increasing pressure.
Fuel cell crossover	Like activation losses
Mass transport	Using oxygen instead of air;
	Prevention of hydrogen pressure drop in cathode;
	Using hydrogen with high purity.
Ohmic crossover	Using electrode with high conductivity;
	Fine and proper plate design;
	Using slim electrode;

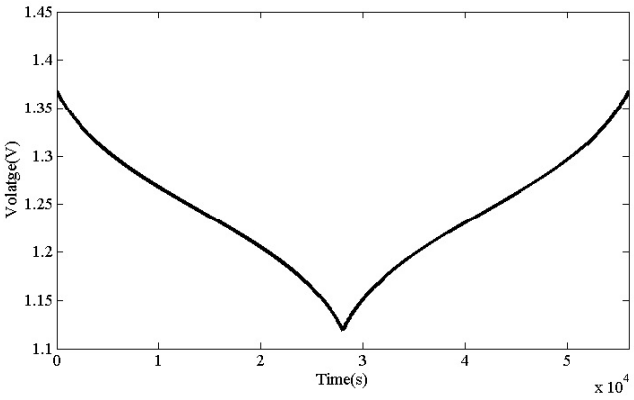

Fig. 5. Modeling result curves of the output voltage in a discharge/charge cycle.

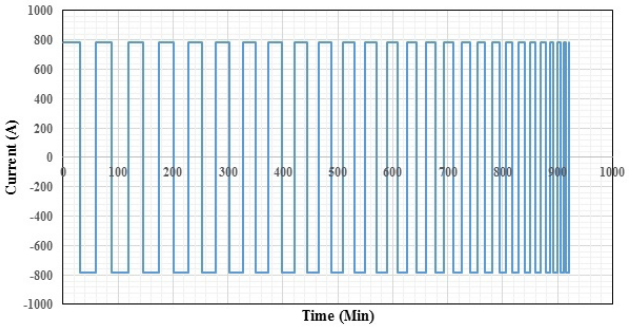

Fig. 6. Modeling result curves of output current in discharge/ charge cycles.

6.2.Concentration change

Activation and ohmic resistance in the electrical circuit are related to ion concentration in the electrolytes [34]. By changing the concentration of the entrance electrolyte the voltage will change. When the V^{2+} and V^{5+} concentration increases, the produced voltage in the discharge situation will also increase; therefore, in charging more voltage is required to reach the desired concentration. The decrease in vanadium concentration in tanks causes a decrease in SOC. The tanks have a higher concentration than cells durng the charging operation. In contrast, in the discharging operation this is the reverse. Therefore, the electrolysis solution is continuously supplied from tanks to cells and voltage increases in charging and decreases in discharging. Fig. 7 shows the concentration change of V^{2+} in during discharge.

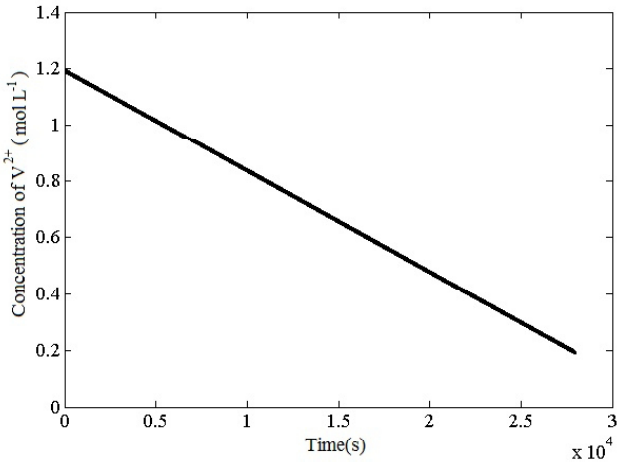

Fig. 7. Concentration change of V^{2+} in discharge mode.

6.3. SOC changes

By calculating SOC the accurate prediction to prevent the increase or decrease of voltage in charge or discharge cycles is done. The amount of SOC can be calculated from OCV amounts. In this experiment, the cell was charged to a maximum voltage of 1.4 V and discharged to a minimum voltage of 1.1 V, which is equivalent to 95% and 10% SOC,

respectively. The SOC rate and therefore the produced electrical power by the battery decreased gradually [29]. At low temperatures, yield will increase because of a decrease of destruction, but at high temperatures the produced energy is higher but destruction is also high. Fig. 8 shows the SOC charge during the discharge cycle according to time.

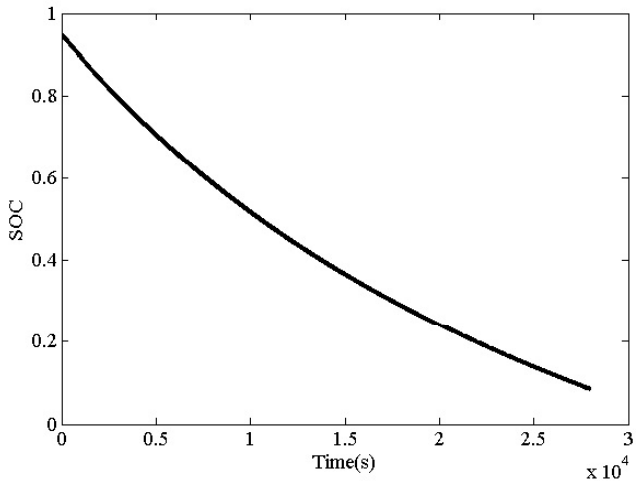

Fig. 8. SOC changes between maximum and minimum limit during discharge.

6.4.Effects of temperature and flow rate

In non-adiabatic conditions, heat loss reduces the temperature in the electrodes and this causes a gradual increase in the cell voltage during the charge cycle and a lower cell voltage during discharge [11]. The stack temperature increases during discharge, but it decreases during the charging process after reaching the steady state.

This is due to smaller cell resistance during the discharge process. By changing the environment temperature the electrolyte temperature will vary.

Variation of temperature in the stack is from –5 to 35°C with constant current density. This indicates that the system works in non-isothermal conditions. The standard potential is temperature dependent and there is a negative linear relationship between them [15]. Temperature effects diffusion of the membrane. The high temperature increases the diffusion rates of vanadium ions through the membrane and therefore the concentrations of active vanadium ions reduces and there is also a reduction of energy in charge-discharge reactions [16]. The ideal work of a fuel cell is related to electrochemical reactions and oxygen. The effects of temperature changes on the charge and discharge operation are indicated in Table 4.

In a PEM fuel cell higher temperature positively affects the reaction kinetics by strongly increasing the charge transform coefficient. At higher temperatures in PEM fuel cells the conductivity of the membrane will increase due to the higher diffusivity.

The flow rate of the electrolyte is an important control mechanism in the operation of a vanadium redox flow battery system. At low flow rates the electrolyte is not efficiently circulated and stagnant regions can form in the electrode. If the flow rate is too high there is a risk of leakage and reaching the sufficient yield will be hard. By increasing flow rate many vanadium species reach into cells and the concentration overpotential will decrease, this results in a high discharge stack voltage and a low charging stack voltage. On the other hand, the charge/discharge cycle is increased under high flow rates. Thus, the capacity of VRB at the same charge/discharge current is increased by high flow rate.

In PEM fuel cells, as mentioned before, the reactant flow non-uniformity will cause the cell voltage to decrease along the stack so the reactant flow and temperature should be balanced in a PEM fuel cell.

7.Conclusion

In distributed generation grids, the amount of achieved energy from a PEM fuel cell at different times of day and year might vary. For this reason, an energy storage system is needed. VRB systems were proposed to charge in 100% of their capacity and have a high yield. This storage omits extended costs and will increase the yield. To analyze VRB cells integrated with PEM fuel cell, a transient model based on electrochemical equations and battery equivalent circuit concept was created as an

Table 4. Temperature changes of VRB systems in different weather conditions.

Climates	Temperature	Charging and discharging	Description
Room temperature	25°C	30 A charging and discharging 30 A charging and 100 A discharging	Temperature rises to 26°C then the electrolyte temperature attains a steady state and oscillates around 26°C. Difference in heat generation rate between charging and discharging is 3 J/s.
		100 A charging and discharging	Temperature increases to 29°C then the electrolyte temperature fluctuates around 31°C. Difference in heat generation rate between charging and discharging is 400 J/s. Temperature increases to 39°C then the electrolyte temperature attains a steady state and oscillates around 26°C. Difference in heat generation rate between charging and discharging is 30 J/s.
Moderate summer climate	15 to 35°C	30 A charging and discharging	The electrolyte temperature reduces and finally oscillates around an equilibrium point of 26°C with the same regular frequency. The difference in heat generation rate between charging and discharging is 3 J/s.
Moderate winter climate	-5 to 15°C	30 A charging and discharging	Stack temperature drops from 15°C to 8°C and it sinusoidal varies around 8°C.

innovative approach to predict cell operation condition.

The results of the model indicated that changes in vanadium concentration in the electrolyte solution affect the output voltage in charge and discharge condition considering the primary concentration of the reactants. The amount of SOC was calculated based on the reactant's changes and the integration of governing equations on both sides of the anode and cathode to control the battery operation during the time. This study has been performed based on a connected fuel cell system consisting of a VRB battery in a PEM fuel cell, a hydrogen ion was used as a reactant and its oxidant is air ions. This study shows that during peak hours 500 W can be achieved from the VEB storage system. This means that approximately 50% of generated energy in the fuel cell can be stored in the VRB battery during low demand conditions. So, this will increase the ion concentration value in the VRB. Moreover, SOC changes to 10% value at nights while in discharge mode and 95% during the day while in charging mode. Eight hours charging in the VRB can produce 4-hour extra electricity to store in the battery. Therefore, during a day 1kW electricity can be produced from the fuel cell, and this portion of generated energy is not required. Finally, the grid can receive 1.5kW power, which it is the principal advantage of the proposed energy generation and storage system.

Nomenclature

E	Stack output voltage
E_0	Cell open circuit voltage at standard pressure
E_{rev}	Theoretical reversible energy
e	Output electrical energy
G	Gibbs free energy
N	Number of cells in stack
n	Number of electrons in reaction

n_o Number of oxygen mole in each fuel mole
RT/nF R is the universal gas constant, F is Faraday's constant, T is the operating temperature and n=2 is the number of transferred electrons in the electrochemical reaction
P_{H2} Partial pressure of hydrogen inside the cell
P_{O2} Partial pressure of oxygen inside the cell
$P_{H2\ OC}$ Partial pressure of gas water
P_{std} Standard pressure
Q Delivered heat
L Voltage losses
i Output current density
i_n Internal current density related to internal current losses
i_0 Exchange current density related to activation losses
i_l Limiting current density related to concentration losses
r Area specific resistance related to resistive losses
ΔC_p Molar heat capacity change

References

[1] Farret, F. A., Simoes, M. G., "Integration of alternative sources of energy", John Wiley & Sons Inc., USA, 2006.

[2] Ogden, J. M., Vielstich, W., Lamm, A., Gasteiger, H.A., "Handbook of Fuel Cells", Wiley, USA, 2003.

[3] Blanchard, J., "Smart Energy Solutions Using Fuel Cells", Telecommunications Energy Conference (INTELEC), IEEE 33rd International, 09 - 13 Oct, Amsterdam, Netherlands, 2011.

[4] Park, J., Li, X., "Effect of flow and temperature distribution on the performance of PEM fuel cell", Journal of Power Sources, 2006, 162:444-459.

[5] Li, Z., Xi, J., Zhou, H., Wu, Z., Qui, X., Chen, L., "Preparation and characterization of sulfonated poly (ether ether krtone)/poly (vinylidene flouride) blend membrane for vanadium redox flow battery application", Journal of Power Sources, 2013, 237:132-140.

[6] Ghadamian, H., Saboohi, Y., "Quantitative analysis of irreversibilities causes voltage drop in fuel cell", Journal of Electrochemica Acta, 2004, 50:699-704.

[7] Ghadamian, H., Bakhtary, Kh., Namini, S. S., "An algorithm for optimum design and macro-model development in PEMFC with exergy and cost considerations", Journal of Power Sources, 2006, 163:87-92.

[8] Kim, J., Lee, S.M., Srinivasan, S., Chamberlin, C.E., "Modeling of Proton Exchange Membrane Fuel Cell Performance with an Empirical Equation", Journal of Electrochemical Society, 1995, 142:2670-2674.

[9] Ceraolo, M., Miulli, C., Pozio, A., "Modelling static and dynamic behaviour of proton exchange membrane fuel cells on the basis of electro-chemical description", Journal of Power Sources, 2003, 113:131-144.

[10] Tang, A., Bao, J., Skyllas-Kazacos, M., "Dynamic modelling of the effects of ion diffusion and side reactions on the capacity loss for vanadium redox flow battery", Power Sources, 2011, 196:10737-10747.

[11] Tang, A., Bao, J., Skyllas-Kazacos, M., "Thermal modelling of battery configuration and self -discharge reactions in vanadium redox flow battery", Power Sources, 2012, 216:489-495.

[12] Skyllas-Kazacos, M., Robbins, R.G., "The All Vanadium Redox Battery", U.S. Patent No. 849 094, 1986.

[13] Heintz, A., Illenberger, C. H., "Thermodynamics of vanadium redox flow batteries – electrochemical and calorimetric investigations", Berichte der Bunsengesellschaft f¨ur physikalische Chemie, 1998, 102:1401-1409.

[14] Shah, A.A., Watt-Smith, M.J., Walsh, F.C., "A dynamic performance model for redox-flow batteries

involving soluble species", Electrochimica Acta, 2008, 53:8087-8100.

[15] Xiong, B., Zhao, J. , Tseng, K.J. ,Skyllas-Kazacos, M., Lim, T. M., Zhang, Y., "Thermal hydraulic behavior and efficiency analysis of an all-vanadium redox flow battery", Power Sources, 2013, 242:314-324.

[16] Sun, C., Tang, Z., Belcher, C., Zawodzinski, T. A., Fujimoto, C., "Evaluation of Diels–Alder poly (phenylene) anion exchange membranes in all-vanadium redox flow batteries", Electrochemistry Communications, 2014, 43:63-66.

[17] Schmal, D., Van Erkel, J., Van Dnin, P. J., "Mass transfer at carbon fibre electrodes", Journal of Applied Electrochemistry, 1986, 16:422-430.

[18] You, D., Zhang, H., Sun, C., Ma, X., "Simulation of the self-discharge process in vanadium redox flow battery", Journal of Power Sources, 2011, 196:1578-1585.

[19] Jiang, R., Derynchu, Z., "Stack design and performance of polymer electrolyte membrane fuel cell", Journal of Power Sources, 2002, 93:25-31.

[20] Mohamed, M. R., Ahmad, H., Abu Seman, M. N. S. Razali, Najib, M. S., "Electrical circuit model of a vanadium redox flow battery using extended Kalman filter", Journal of Power Sources, 2013, 239:284-293.

[21] Skyllas-Kazacos, M., Kazacos, M., "State of charge monitoring methods for vanadium redox flow battery control", Journal of Power Sources, 2011, 196:8822-8827.

[22] Ozgoli, H. A., Elyasi, S., "Hydrodynamic and electrochemical modeling of vanadium redox flow battery", Mechanics & Industry, 2015, 16:1.

[23] Ozgoli, H. A., Elyasi, S., "A transient model of vanadium redox flow battery", Mechanics & Industry, 2016, 17:1-13.

[24] Andrea, E., Ma˜nana, M., Ortiz, A., Renedo, C., Egu´ıluz, L., P´erez, S., Delgado, F., "A simplified electrical model of small PEM fuel cell", Renewable Energy & Power Quality Journal, 2006, 1:281-284.

[25] You, D., Zhang, H., Chen, J., "A simple model for the vanadium redox battery", Electrochimica Acta, 2009, 54:6827-6836.

[26] Al-Fetlawi, H., Shah A. A., Walsh, F. C., "Non-isothermal modelling of the all-vanadium redox flow battery", Electrochim Acta, 2009, 55:78-89.

[27] Skyllas-Kazacos, M., Kazacos, M., "State of charge monitoring methods for vanadium redox flow battery control", Journal of Power Sources, 2011, 196:8822-8827.

[28] Skyllas-Kazacos, M., Chakrabarti, M. H., S. Hajimolana, A. , Mjalli, F. S., Saleem, M., "Progress in Flow Battery Research and Development", Journal of the Electrochemical Society, 2011, 158:1-25.

[29] Corcuera, S., Skyllas-Kazacos, M., "State-Of-Charge Monitoring and Electrolyte Rebalancing Methods for the Vanadium Redox Flow Battery", European Chemical Bulletin, 2012, 1:511-519.

[30] Sukkar, T., Skyllas-Kazacos, M., "Water transfer behaviour across cation exchange membranes in the vanadium redox battery", Journal of Membrane Science, 2003, 222:235-247.

[31] Tomadakis, M., Robertson, T. J., "Viscous permeability of random fiber structures: comparison of electrical and diffusional estimates with experimental and analytical results" Journal of Composite Materials, 2005, 39:163-188.

[32] Chen, S. X., Gooi, H. B., Xia, N., "Modelling of lithium-ion battery for online energy management systems", Electrical Systems in Transportation, 2012, 2:202-210.

[33] Binyu, X., Zhao, J., Zhongbao, W., Chenda, Z., "State of Charge Estimation of an All-Vanadium Redox

Flow Battery Based on a Thermal-Dependent Model", Power and Energy Engineering Conference (APPEEC), 2013:1-6.

[34] Wen, Y., Zhang, H., Qian, P., Zhao, P., Zhou, H., Yi, B., "Investigations on the Electrode Process of Concentrated V(IV)/V(V) Species in a Vanadium Redox Flow Battery", Acta Physico-Chimica Sinica, 2006, 22:403-408.

[35] Li, Z., Xi, J., Zhou, H., Wu, Z., Qui, X., Chen, L., "Preparation and characterization of sulfonated poly (ether ether krtone)/poly (vinylidene flouride) blend membrane for vanadium redox flow battery application", Journal of Power Sources, 2013, 237:132-140.

[36] Guvelioglu, G. H., Stenger, H. G., "Computational fluid dynamics modeling of polymer electrolyte membrane fuel cells", Journal of Power Sources, 2005, 147:95-106.

[37] Barnes, F. S., "Cell membrane temperature rate sensitivity predicted from nerst equation", bio electro magnetics, 1984, 5:113-115.

[38] Knehr, K. W., Agar, E., Dennison, C. R., Kalidindi, A. R., Kumbur, E. C., "A Transient Vanadium Flow Battery Model Incorporating Vanadium Crossover and Water Transport through the Membrane", Journal of The Electrochemical Society, 2012, 159:A1446-A1459.

[39] Coppo, M., Siegel, N. P., Von Spakovsky, M. R., "On the influence of temperature on PEM fuel cell operation" Journal of Power Sources, 2006, 159:560-569.

[40] Park, J., Li, X., "Effect of flow and temperature distribution on the performance of PEM fuel cell", Journal of Power Sources, 2006, 162:444-459.